Original Article

Potential clinical feasibility of synthetic MRI in bladder tumors: a comparative study with conventional MRI

Meiqin Li[1#^], Wenhao Fu[1#^], Longyuan Ouyang[1], Qian Cai[1^], Yiping Huang[1^], Xiaoyu Yang[1], Weibin Pan[1], Long Qian[2], Yan Guo[1^], Huanjun Wang[1^]

[1]Department of Radiology, The First Affiliated Hospital, Sun Yat-sen University, Guangzhou, China; [2]MR Research, GE Healthcare, Beijing, China

Contributions: (I) Conception and design: Y Guo, H Wang, M Li, W Fu; (II) Administrative support: H Wang; (III) Provision of study materials or patients: Y Guo, H Wang, Q Cai; (IV) Collection and assembly of data: L Ouyang, Q Cai, Y Huang, X Yang, W Pan, L Qian; (V) Data analysis and interpretation: Y Guo, H Wang, M Li, W Fu; (VI) Manuscript writing: All authors; (VII) Final approval of manuscript: All authors.

[#]These authors contributed equally to this work and should be considered as co-first authors.

Correspondence to: Yan Guo, PhD; Huanjun Wang, PhD. Department of Radiology, The First Affiliated Hospital, Sun Yat-sen University, 58 Zhongshan Road 2, Guangzhou 510030, China. Email: gyan@mail.sysu.edu.cn; wanghj45@mail.sysu.edu.cn.

Background: Synthetic magnetic resonance imaging (MRI) can provide quantitative information about inherent tissue properties and synthesize tailored contrast-weighted images simultaneously in a single scan. This study aimed to investigate the clinical feasibility of synthetic MRI in bladder tumors.

Methods: A total of 47 patients (37 males; mean age: 66±10 years old) with postoperative pathology-confirmed papillary urothelial neoplasms of the bladder were enrolled in this retrospective study. A 2-dimensional (2D) multi-dynamic multi-echo pulse sequence was performed for synthetic MRI at 3T. The overall image quality, lesion conspicuity, contrast resolution, resolution of subtle anatomic structures, motion artifact, blurring, and graininess of images were subjectively evaluated by 2 radiologists independently using a 5-point Likert scale for qualitative analysis. The signal intensity ratio (SIR), signal-to-noise ratio (SNR), and contrast-to-noise ratio (CNR) were measured for quantitative analysis. Linear weighted Kappa, Wilcoxon's signed-rank test, and the Mann–Whitney U-test were used for statistical analysis.

Results: The interobserver consistency was excellent (κ values: 0.607–1). Synthetic T1-weighted (syn-T1w) and synthetic T2-weighted (syn-T2w) images obtained scores of 4 in most subjective terms, which were relatively smaller than those of conventional images. The SIR and SNR of syn-T1w were significantly higher than those of con-T1w images (SIR 2.37±0.86 *vs.* 1.47±0.20, P<0.001; SNR 21.83±9.43 *vs.* 14.81±3.30, P<0.001). No difference was found in SIR between syn-T2w and conventional T2-weighted (con-T2w) images, whereas the SNR of the syn-T2w was significantly lower (8.79±4.06 *vs.* 26.49±6.80, P<0.001). Additionally, the CNR of synthetic images was significantly lower than that of conventional images (T1w 1.41±0.72 *vs.* 2.68±1.04; T2w 1.40±0.87 *vs.* 4.03±1.55, all P<0.001).

Conclusions: Synthetic MRI generates morphologic magnetic resonance (MR) images with diagnostically acceptable image quality in bladder tumors, especially T1-weighted images with high image contrast of tumors relative to urine. Further technological improvements are needed for synthetic MRI to reduce noise. Combined with T1, T2, and proton density (PD) quantitative data, synthetic MRI has potential for clinical application in bladder tumors.

Keywords: Synthetic magnetic resonance imaging (synthetic MRI); bladder tumor; image quality

^ ORCID: Meiqin Li, 0000-0002-3063-5758; Wenhao Fu, 0000-0001-7232-6243; Qian Cai, 0000-0001-5671-7885; Yiping Huang, 0000-0001-9884-9472; Yan Guo, 0000-0002-0267-7328; Huanjun Wang, 0000-0001-9089-7736.

Submitted Dec 21, 2022. Accepted for publication May 19, 2023. Published online May 31, 2023.
doi: 10.21037/qims-22-1419
View this article at: https://dx.doi.org/10.21037/qims-22-1419

Introduction

Bladder cancer (BC), a disease predominantly affecting older males, is the 9th most common malignant tumor worldwide, with approximately 540,000 new cases and 200,000 deaths per year (1). Magnetic resonance imaging (MRI) has been widely used in the preoperative staging evaluation for BC in recent years, especially since the introduction of the bladder Vesical Imaging-Reporting and Data System (VI-RADS) in 2018, in which a standardized image acquisition and reporting system were recommended (2). Conventionally, multiparametric MRI, including T1-weighted imaging (T1W), T2-weighted imaging (T2W), diffusion-weighted imaging (DWI), and dynamic contrast-enhanced images, has been applied in preoperative evaluations for staging and postoperative follow-up (3,4). Contrastingly, conventional MRI, especially T1W and T2W images, only supplies qualitative information based on signal intensity, not objective and quantitative data for diagnosis. A previous study reported that the T1, T2, and proton density (PD) values could be used in the preoperative evaluation of BC grade, which were significantly lower in high-grade BC than in low-grade BC (5). However, extra scanning time is needed to obtain these quantitative parameters beyond the acquisition of conventional sequences.

Synthetic MRI, a simultaneous relaxometry technique, maps the properties of physical tissues, such as longitudinal T1 and transverse T2 relaxation times, PD, and the amplitude of the local radio frequency. It then generates multiple contrast images based on the tissue properties through mathematical reference in a single scan (6,7). In this context, synthetic MRI can provide quantitative information about inherent tissue properties, which is helpful for characterizing lesions and monitoring disease progression and synthesizing tailored contrast-weighted images simultaneously. Previous studies have demonstrated that synthetic MRI scans are acceptable substitutes for conventional MRI scans for neuroimaging in children and adults, but with a shorter scan time, and could be feasible for routine clinical use in daily practice (6,8-11). In these studies, synthetic MRI was suggested as an alternative imaging method in multiple sclerosis based on its ability to perform tissue segmentation and volumetric assessment for intracranial tissue components (12-14). It has also been shown to achieve comparable image quality to conventional MRI when applied to the knee joint and lamellar spine (15,16). Additionally, relaxation maps derived from synthetic MRI have been reported to be helpful for effectively distinguishing malignant lesions from benign pathologies in the breast and prostate (17-21). Notably, our previous work explored whether synthetic quantitative parameters could improve BC grading and staging from the perspective of diagnostic efficiency (5). However, few studies have evaluated the image quality of synthetic MRI in bladder imaging from the technical perspective. Thus, our study aimed to investigate the clinical feasibility of synthetic MRI in bladder tumors by comparing its image quality to that of conventional MRI.

Methods

Patients

The study was conducted in accordance with the Declaration of Helsinki (as revised in 2013). The study was approved by the Ethics Committee of the First Affiliated Hospital of Sun Yat-sen University and individual consent for this retrospective analysis was waived. Patients with suspected bladder lesions were enrolled consecutively from June to December 2020. The inclusion criteria were as follows: (I) clinical suspicion of bladder tumor; (II) MRI examination within 2 weeks prior to surgical treatment; (III) postoperative pathologically confirmed papillary urothelial neoplasms and grading. Patients with tumors smaller than 10 mm in diameter and MRI contraindications were excluded from the study. A total of 73 patients were recruited into this study. However, 5 patients were excluded because of the lack of surgical treatment, and 15 patients were excluded due to smaller tumor diameters. A further 6 patients were excluded based on their pathological results (1 endometriosis, 2 inflammatory polyps, 1 glandular cystitis, and 2 ureteral carcinomas). Finally, 47 patients (37 male patients; mean age: 66±10 years old; age range: 31–82 years) matched our inclusion and exclusion criteria, and were enrolled in this study. Specifically, 34 patients underwent transurethral resection, 11 proceeded to radical cystectomy, and 2 received neoadjuvant chemotherapy. The pathological grade distribution was as follows: high grade

Table 1 Criteria of qualitative assessment of image quality in MR images in patients with bladder tumors

Likert score	Overall image quality	Lesion conspicuity; visual grayscale contrast; spatial resolution	Motion artifact; graininess; blurring
1	Nondiagnostic	Nondiagnostic	Severe
2	Insufficient quality for diagnosis	Poor	Moderate
3	Sufficient but with perceptible image degradations	Satisfactory	Mild
4	Only minor image degradations	Good	Slight
5	No image degradations	Excellent	None

MR, magnetic resonance.

(29 patients), low grade (13 patients), papillary urothelial neoplasms with low malignant potential (3 patients), and papillary urothelial neoplasms with uncertain malignant potential (2 patients). The tumor sizes ranged from 11 to 76 mm (mean: 28.6±17.5 mm).

MRI

All the MR examinations were performed with a 3-T scanner (Discovery MR750W; GE Healthcare, Waukesha, WI, USA) using a standard body coil [General Electric Medical (GEM) anterior array coil] and adopting a feet-first orientation. The synthetic sequences were acquired after conventional non-contrast sequences during clinical MRI examinations for patients suspected of having bladder tumors. A 2-dimensional (2D) multi-dynamic, multi-echo (MDME) pulse sequence, dynamically combining 4 automatically calculated saturation delay times and 2 echo times (TEs), was performed (scan time: 6 min, 8 s) at axial sections for synthetic MRI. The parameters of the MDME sequence were as follows: repetition time (TR) =4,000 ms, TE =16.9/92.8 ms, the field of view (FOV) =220 mm, matrix =320×256, section thickness =4 mm, slice gap =1 mm, echo train length =16, bandwidth =41.67 Hz, acceleration factor =2, and the number of excitations (NEX) =1. The synthetic T1-weighted (syn-T1w) and synthetic T2-weighted (syn-T2w) images were generated from the MDME raw data using TE/TR values (10 ms/500 ms, 100 ms/4,500 ms) in postprocessing software (v8.0.4; Synthetic MR, Linkoping, Sweden). Imaging parameters (TR, TE) were selected to provide similar visual image contrast to the conventional MR images.

Then, an axial fast spin-echo sequence for the conventional T1-weighted (con-T1w) images was performed (scan time: 2 min, 3 s) with the following parameters: TR =758 ms, TE =12 ms, flip angle =111°, FOV =220 mm, matrix =352×320, section thickness =4 mm, slice gap =1 mm, and NEX =2. An axial periodically rotated overlapping parallel lines with enhanced reconstruction (PROPELLER) sequence for the conventional T2-weighted (con-T2w) images was acquired in 2 minutes and 10 seconds with the following parameters: TR =4,175 ms, TE =106.2 ms, flip angle =110°, FOV =220 mm, matrix =384×250, section thickness =4 mm, slice gap =1 mm, and NEX =2.5. The scanning range and center were maintained to be consistent across all the above for each patient.

Qualitative analysis

The synthetic and conventional images were independently evaluated by 2 radiologists (Weibin Pan and Xiaoyu Yang, with at least 10 years of experience in abdominal MRI), who were aware of the presence of a bladder tumor but blinded to whether they were synthetic or conventional images. A 5-score Likert scale was used for assessment in terms of the following: (I) overall image quality; (II) lesion conspicuity representing the ability to exhibit a lesion relative to the background urine (22); (III) contrast resolution defined as the ability to detect subtle differences in grayscale in images (23); (IV) spatial resolution demonstrating the subtle anatomic structures in the pelvic region; (V) motion artifact; (VI) graininess; (VII) blurring, judged by whether the normal bladder wall was distinguishable (*Table 1*).

Quantitative analysis

Quantitative analysis was performed using ITK-SNAP software (Version 3.6.0; http://www.itksnap.org/pmwiki/pmwiki.php) in a double-blind manner (24). Since images in the 2 groups (synthetic and conventional T1W images,

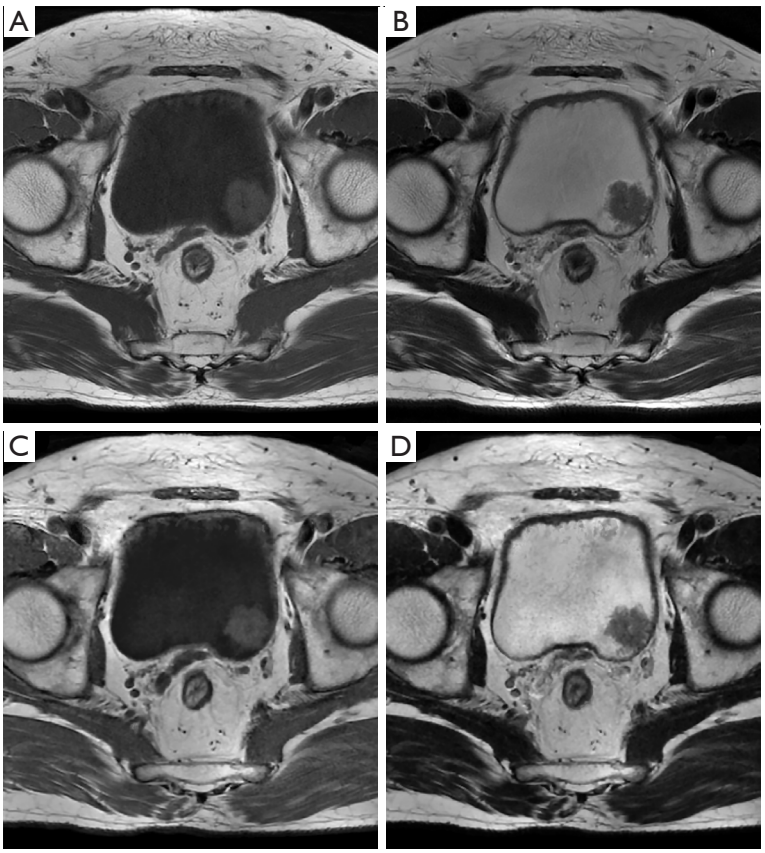

Figure 1 Conventional and synthetic T1, T2 weighted images in bladder tumors. A 71-year-old male with postoperative pathology confirmed low-grade papillary urothelial neoplasms of the bladder. (A) Conventional T1-weighted images. (B) Conventional T2-weighted images. (C) Synthetic T1-weighted images. (D) Synthetic T2-weighted images.

T2W images) were loaded simultaneously and had the same scan range, slice thickness, and gap for these sequences, the tumors were displayed in the same position (*Figure 1*). When multiple tumors were detected, the largest single tumor was analyzed. The regions of interests (ROIs) were manually drawn by a radiologist (Meiqin Li) to profile the tumor on the layer with the largest tumor size, avoiding necrosis, artifacts, blood vessels, and so on, which was further checked on the dynamic contrast-enhanced T1W image. In the same layer, an ROI of the urine was delineated using unified circular sampling (voxel count =300). Then, the mean signal amplitude of the tumor (SI_{tumor}) and its standard deviation (σ_{tumor}) of the images were recorded, as well as those of the urine (SI_{urine}) and (σ_{urine}), for each patient. Finally, the signal intensity ratio (SIR) was calculated using Eq. [1].

$$SIR = \frac{SI_{tumor}}{SI_{urine}} \quad [1]$$

The relative signal-to-noise ratio (SNR) was calculated as Eq. [2].

$$SNR = \frac{SI_{tumor}}{\sigma_{urine}} \quad [2]$$

Furthermore, the contrast-to-noise ratio (CNR) was quantified using Eq. [3] (25,26).

$$CNR = \frac{\left|SI_{tumor} - SI_{urine}\right|}{\sqrt{\sigma_{tumor}^{2} + \sigma_{urine}^{2}}} \quad [3]$$

Statistical analysis

All the statistical analyses were performed using SPSS software, version 26 (IBM Corp., Armonk, NY, USA). For qualitative analysis, the interobserver agreement was evaluated using the linear weighted Kappa statistics and interpreted as follows: slight agreement (0–0.20), fair agreement (0.21–0.40), moderate agreement (0.41–0.60), substantial agreement (0.61–0.80), and excellent agreement (0.81–1.00) (22). Differences in subjective scores between

Table 2 Interobserver agreement of qualitative assessment for MR images in patients with bladder tumors

Variables	Con MRI		Syn MRI	
	T1	T2	T1	T2
Overall image quality	0.643	1	0.649	0.853
Lesion conspicuity	0.607	0.647	0.925	0.647
Motion artifact	0.796	0.785	0.666	0.645
Blurring	0.756	0.674	0.766	0.797
Graininess	0.757	0.897	0.633	0.883
Visual grayscale contrast	0.737	0.846	0.942	0.732
Resolution of subtle anatomic structures	0.65	0.728	0.811	0.901

Data listed is the weighted kappa values. MR, magnetic resonance; Con MRI, conventional magnetic resonance imaging; Syn MRI, synthetic magnetic resonance imaging.

Table 3 Qualitative comparison between conventional and synthetic T1-weighted images in patients with bladder tumors

Variables	Observer 1			Observer 2		
	Con MRI	Syn MRI	P	Con MRI	Syn MRI	P
Overall image quality	5 [4–5]	4 [4–4]	*	5 [5–5]	4 [4–4]	*
Lesion conspicuity	4 [4–5]	4 [4–5]	0.464	5 [4–5]	4 [4–5]	0.004
Motion artifact	4 [4–5]	4 [4–5]	0.97	4 [4–5]	4 [4–5]	0.6
Blurring	5 [4–5]	4 [4–4]	0.017	5 [4–5]	4 [4–5]	0.01
Graininess	5 [5–5]	4 [4–4]	*	5 [5–5]	4 [4–4]	*
Visual grayscale contrast	5 [5–5]	4 [4–5]	*	5 [5–5]	4 [4–4]	*
Resolution of subtle anatomic structures	5 [5–5]	5 [4–5]	0.18	5 [5–5]	5 [4–5]	0.001

Data expressed as the median [first quartile and third quartile]. *, P<0.001. Con MRI, conventional magnetic resonance imaging; Syn MRI, synthetic magnetic resonance imaging.

the conventional and synthetic groups (T1w and T2w images) were assessed using Wilcoxon's signed-rank test. The SIR, SNR, and CNR were compared using the Mann-Whitney U test. A P value <0.05 indicated a statistically significant difference.

Results

Qualitative analysis of imaging quality

Interobserver agreement ranged from substantial to excellent (weighted kappa values: 0.607–1) for all image features (*Table 2*). Comparison data between synthetic and conventional MRI are summarized in *Tables 3*,*4*. For syn-T1w images, the subjective scores of image features were all 4 points, except for that of spatial resolution, which was 5 points. There was no difference between syn-T1w and con-T1w images regarding lesions' conspicuity, motion artifact, and spatial resolution (all P>0.05). However, the subjective scores of overall image quality, blurring, graininess, and contrast resolution of syn-T1w were lower than those of the con-T1w images (all P<0.05) (*Table 3*). Similarly, for syn-T2w images, the average subjective scores of the lesion conspicuity and spatial resolution were 5 points, whereas other image quality features were 4 points consistently. Moreover, the subjective scores for syn-T2w images were significantly lower than those for con-T2w images (all P<0.01) (*Table 4*).

Quantitative analysis of imaging quality

For syn-T1w images, the SIR was significantly higher than

Table 4 Qualitative comparison between conventional and synthetic T2-weighted images in patients with bladder tumors

Variables	Observer 1			Observer 2		
	Con MRI	Syn MRI	P	Con MRI	Syn MRI	P
Overall image quality	5 [5–5]	4 [4–5]	*	5 [5–5]	4 [4–4]	*
Lesion conspicuity	5 [5–5]	5 [4–5]	0.001	5 [5–5]	5 [4–5]	0.002
Motion artifact	5 [5–5]	4 [4–5]	*	5 [5–5]	4 [4–5]	*
Blurring	5 [5–5]	4 [4–5]	*	5 [5–5]	4 [4–5]	*
Graininess	5 [5–5]	4 [4–4]	*	5 [5–5]	4 [4–4]	*
Visual grayscale contrast	5 [5–5]	4 [4–4]	*	5 [5–5]	4 [4–4]	*
Resolution of subtle anatomic structures	5 [5–5]	5 [4–5]	*	5 [5–5]	5 [4–5]	0.008

Data expressed as the median [first quartile and third quartile]. *, P<0.001. Con MRI, conventional magnetic resonance imaging; Syn MRI, synthetic magnetic resonance imaging.

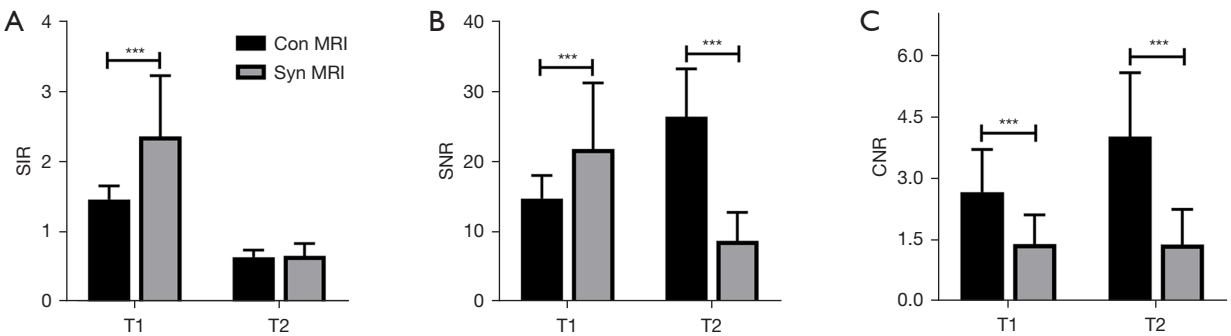

Figure 2 Quantitative comparisons of images between conventional and synthetic MRI in patients with bladder tumors. (A) SIR; (B) SNR; (C) CNR. ***, P<0.001. SIR, signal intensity ratio; SNR, signal-to-noise ratio; CNR, contrast-to-noise ratio; Con MRI, conventional magnetic resonance imaging; Syn MRI, synthetic magnetic resonance imaging.

that of con-T1w images (2.37±0.86 *vs.* 1.47±0.20, P<0.001), as well as the SNR (21.83±9.43 *vs.* 14.81±3.30, P<0.001). However, the CNR was significantly lower in syn-T1w images (1.41±0.72 *vs.* 2.68±1.04, P<0.001). For syn-T2w images, no significant difference in the SIR was found compared to con-T2w images (0.67±0.18 *vs.* 0.65±0.10, P=0.794), whereas the SNR and CNR were significantly lower than that of con-T2w images (SNR: 8.79±4.06 *vs.* 26.49±6.80, CNR: 1.40±0.87 *vs.* 4.03±1.55, P<0.001) (*Figure 2*).

Discussion

Synthetic MRI, a high-profile imaging technology, has gained widespread attention for increasing the efficiency of examinations. This study was the first to explore its potential clinical application in bladder tumors with qualitative and quantitative image quality comparisons to conventional MRI. The results demonstrated high subjective scores in all of image features of syn-T1w and syn-T2w images, although lower than those of conventional MRI. The quantitative analysis showed a higher SIR/SNR and a lower CNR of syn-T1w images. However, the SIR, SNR, and CNR were inferior on syn-T2w images.

Synthetic MRI quantifies T1, T2, PD, and B1 field values in a single acquisition. Based on the quantitative values, tailored contrast-weighted images, such as T1, T2, PD, T1-weighted-fluid attenuated inversion recovery (T1 Flair), T2 Flair, and short T1 inversion recovery (STIR)-weighted images, can be synthesized by post processing. The main sequences we focused on in this study were the T1- and T2-weighted images since they are conventionally included for bladder MR images in clinical practice. In the present study, the concordance rate was substantial and

excellent between the 2 observers in evaluating the image quality of synthetic MRI, indicating that image features were user-friendly and easy to understand and suggesting that synthetic MRI was stable and reproducible. Moreover, syn-T1w and syn-T2w images achieved a score greater or equal to 4 in all the qualitatively evaluated terms, suggesting sufficient image quality with minor degradations for diagnosis. The relatively high-definition bladder MR images with a small FOV enabled a clear presentation of details and more detailed observation of lesions. Based on their clinical experience, both observers gave con-T1w and con-T2w images almost 5 points overall according to the assessment criteria and gave that of syn-T1w and syn-T2w images almost 4 points overall. From the perspective of the central tendency of scores, the qualitative analysis presented a low discrimination capability. However, the between-group comparisons revealed significant differences in most characteristics of images. Although the subjective scores of synthetic T1- and T2-weighted images were lower than that of conventional ones, the image quality of synthetic MR images was diagnostically acceptable. Further technological improvements are needed for synthetic MRI to achieve comparable and alternative image quality. Additionally, the inclusion of the Turing test in future studies will increase the integrity of qualitative analysis (27).

Additionally, the subjective scores of motion artifact on conventional T2W images were higher than that on synthetic images. This result benefits from the PROPELLER technique, a radial k-space sampling concept that enables correction of motion artifacts (28). However, the synthetic sequence is very sensitive to motion to obtain a correct reconstruction. From the images shown, motion artifacts were mainly found in the anterior portion of the bladder, which could result from the body coil moving with the respiratory system. This point may be addressed by suitable body coil placement in future works.

Furthermore, syn-T1w images yielded a significantly higher SIR, for which the tumors were more clearly presented as contrasted against the surrounding urine. Besides, the SNR was also relatively superior on syn-T1w images but inferior on syn-T2w images. In addition, the CNR of synthetic images was relatively lower than that of conventional MRI, suggesting a higher noise level. This finding could be explained by the algorithm and the parameter selection of the synthetic sequences. Synthetic MRI generates multiple image contrasts based on the tissue properties by dynamically combining TR, TE, and inversion time (TI) values, rather than predetermining scan parameters (6). In contrast, other scan parameters could influence the SNR and CNR, such as FOV, matrix size, and slice thickness (29). Using a lower number of NEX in synthetic sequence or the characteristics of the PROPELLER sequence may be reasons for lower SNR and CNR in syn-T2w images. The relatively lower qualitative score of synthetic images was due to high noise. A previous study performed on the brain reported a similar noise level result, which revealed an acceptable image quality for the diagnosis (8). In future, further technique-refining efforts could be directed toward the current noise level, although it causes subtle effects on the diagnosis.

From a diagnostic perspective, the syn-T1w images displayed better image quality than the syn-T2w images in this study. Although T2W is the key the recommended image protocol for VI-RADS, T1W is a common and indispensable component used to identify hemorrhage and clots in the bladder, and bone metastasis (2). More importantly, synthetic MRI provides the absolute T1, T2, and PD values of the properties of physical tissues. Specifically, synthetic mapping (T1, T2, and PD) can quantify bone marrow edema and fat metaplasia (30). Synthetic relaxometry could discriminate acute and chronic ischemic lesions (31). Remarkably, our previous work revealed that synthetic MRI-derived parameters could be used in the preoperative evaluation of bladder tumor grade; the T1, T2, and PD values were significantly lower in high-grade BC than low-grade BC (5). Additionally, although it appears that the scanning time of synthetic MRI is longer than that of conventional T1- and T2-weighted images, synthetic MRI generates quantitative maps synchronously without extra time for special quantitative sequences, potentially reducing the entire scanning time. Combined with its quantitative values and satisfactory image quality, synthetic MRI is promising for bladder imaging.

The study had several limitations. First, only cross-sectional images of conventional and synthetic MRI were compared. In contrast, the current clinical setting was a multi-directional (transverse, coronal, sagittal, or any angle) section showing the anatomy and bladder tumors. However, there was no difference in overall interobserver consistency in the axial plane. Further studies containing coronal and/or sagittal planes are necessary. Second, considering the impact of partial volume effects, tumors smaller than 10 mm in diameter were excluded. Thus, observer selection bias might exist, which could have affected the analysis and should also be considered. Third, imaging parameters (TR, TE, and TI) were selected to provide similar visual image contrast

to conventional images. In the present study, synthetic MR images were optimized as tissue-stressed T2W images as much as possible, which could provide optimal diagnostic performance. Furthermore, the same TR and TE did not necessarily produce the same image contrast (15), yet, the quantitative analysis may be undeniably affected by the different parameterizations. Finally, assessing diagnostic accuracy is essential to study the clinical feasibility of a new technique. However, the results showed that the synthetic images had diagnostically acceptable image quality and good lesion conspicuity ability. Besides, the contrast-enhanced T1W is clinically essential but was not incorporated into the comparations. Further research is needed to explore the diagnostic efficiency for BC using synthetic MRI.

Conclusions

In conclusion, synthetic MRI generates morphologic MR images with diagnostically acceptable image quality in bladder tumors, especially T1W images with high image contrast of tumors relative to urine. Further technological improvements are needed for synthetic MRI to reduce noise. Combined with the T1, T2, and PD quantitative data, synthetic MRI has good potential for clinical application in bladder tumors.

Acknowledgments

Funding: This work was supported by the National Natural Science Foundation of China (No. 82071989), Natural Science Foundation of Guangdong Province (No. 2021A1515012243), the 2021 SKY Imaging Science and Research Fund of China International Medical Foundation (No. Z-2014-07-2101-12), and the Kelin New Star Talent Program of the First Affiliated Hospital of Sun Yat-sen University (No. R08028).

Footnote

Conflicts of Interest: All authors have completed the ICMJE uniform disclosure form (available at https://qims.amegroups.com/article/view/10.21037/qims-22-1419/coif). LQ is a consultant of GE Healthcare China. The other authors have no conflicts of interest to declare.

Ethical Statement: The authors are accountable for all aspects of the work in ensuring that questions related to the accuracy or integrity of any part of the work are appropriately investigated and resolved. The study was conducted in accordance with the Declaration of Helsinki (as revised in 2013). The study was approved by the Institutional Ethics Committees of the First Affiliated Hospital of Sun Yat-sen University and individual consent for this retrospective analysis was waived.

References

1. Antoni S, Ferlay J, Soerjomataram I, Znaor A, Jemal A, Bray F. Bladder Cancer Incidence and Mortality: A Global Overview and Recent Trends. Eur Urol 2017;71:96-108.
2. Panebianco V, Narumi Y, Altun E, Bochner BH, Efstathiou JA, Hafeez S, Huddart R, Kennish S, Lerner S, Montironi R, Muglia VF, Salomon G, Thomas S, Vargas HA, Witjes JA, Takeuchi M, Barentsz J, Catto JWF. Multiparametric Magnetic Resonance Imaging for Bladder Cancer: Development of VI-RADS (Vesical Imaging-Reporting And Data System). Eur Urol 2018;74:294-306.
3. Delli Pizzi A, Mastrodicasa D, Marchioni M, Primiceri G, Di Fabio F, Cianci R, Seccia B, Sessa B, Mincuzzi E, Romanelli M, Castellan P, Castellucci R, Colasante A, Schips L, Basilico R, Caulo M. Bladder cancer: do we need contrast injection for MRI assessment of muscle invasion? A prospective multi-reader VI-RADS approach. Eur Radiol 2021;31:3874-83.
4. Wang Y, Chen S, Zhang W, Xiao W, Su J, Zhang R, Wei Y, Luo M. Image quality evaluation of diffusion-weighted imaging in bladder cancer: a comparison between integrated slice-specific dynamic shimming and single-shot echo-planar imaging. Quant Imaging Med Surg 2023;13:2526-37.
5. Cai Q, Wen Z, Huang Y, Li M, Ouyang L, Ling J, Qian L, Guo Y, Wang H. Investigation of Synthetic Magnetic Resonance Imaging Applied in the Evaluation of the Tumor Grade of Bladder Cancer. J Magn Reson Imaging 2021;54:1989-97.
6. Warntjes JB, Leinhard OD, West J, Lundberg P.

Rapid magnetic resonance quantification on the brain: Optimization for clinical usage. Magn Reson Med 2008;60:320-9.
7. Warntjes JB, Dahlqvist O, Lundberg P. Novel method for rapid, simultaneous T1, T2*, and proton density quantification. Magn Reson Med 2007;57:528-37.
8. Blystad I, Warntjes JB, Smedby O, Landtblom AM, Lundberg P, Larsson EM. Synthetic MRI of the brain in a clinical setting. Acta Radiol 2012;53:1158-63.
9. Ryu KH, Baek HJ, Moon JI, Choi BH, Park SE, Ha JY, Jeon KN, Bae K, Choi DS, Cho SB, Lee Y, Heo YJ. Initial clinical experience of synthetic MRI as a routine neuroimaging protocol in daily practice: A single-center study. J Neuroradiol 2020;47:151-60.
10. Andica C, Hagiwara A, Hori M, Kamagata K, Koshino S, Maekawa T, Suzuki M, Fujiwara H, Ikeno M, Shimizu T, Suzuki H, Sugano H, Arai H, Aoki S. Review of synthetic MRI in pediatric brains: Basic principle of MR quantification, its features, clinical applications, and limitations. J Neuroradiol 2019;46:268-75.
11. Betts AM, Leach JL, Jones BV, Zhang B, Serai S. Brain imaging with synthetic MR in children: clinical quality assessment. Neuroradiology 2016;58:1017-26.
12. Hagiwara A, Warntjes M, Hori M, Andica C, Nakazawa M, Kumamaru KK, Abe O, Aoki S. SyMRI of the Brain: Rapid Quantification of Relaxation Rates and Proton Density, With Synthetic MRI, Automatic Brain Segmentation, and Myelin Measurement. Invest Radiol 2017;52:647-57.
13. Granberg T, Uppman M, Hashim F, Cananau C, Nordin LE, Shams S, Berglund J, Forslin Y, Aspelin P, Fredrikson S, Kristoffersen-Wiberg M. Clinical Feasibility of Synthetic MRI in Multiple Sclerosis: A Diagnostic and Volumetric Validation Study. AJNR Am J Neuroradiol 2016;37:1023-9.
14. Cao J, Xu X, Zhu J, Wu P, Pang H, Fan G, Cui L. Rapid quantification of global brain volumetry and relaxometry in patients with multiple sclerosis using synthetic magnetic resonance imaging. Quant Imaging Med Surg 2022;12:3104-14.
15. Yi J, Lee YH, Song HT, Suh JS. Clinical Feasibility of Synthetic Magnetic Resonance Imaging in the Diagnosis of Internal Derangements of the Knee. Korean J Radiol 2018;19:311-9.
16. Zhang W, Zhu J, Xu X, Fan G. Synthetic MRI of the lumbar spine at 3.0 T: feasibility and image quality comparison with conventional MRI. Acta Radiol 2020;61:461-70.
17. Gao W, Zhang S, Guo J, Wei X, Li X, Diao Y, Huang W, Yao Y, Shang A, Zhang Y, Yang Q, Chen X. Investigation of Synthetic Relaxometry and Diffusion Measures in the Differentiation of Benign and Malignant Breast Lesions as Compared to BI-RADS. J Magn Reson Imaging 2021;53:1118-27.
18. Cui Y, Han S, Liu M, Wu PY, Zhang W, Zhang J, Li C, Chen M. Diagnosis and Grading of Prostate Cancer by Relaxation Maps From Synthetic MRI. J Magn Reson Imaging 2020;52:552-64.
19. Meng T, He N, He H, Liu K, Ke L, Liu H, Zhong L, Huang C, Yang A, Zhou C, Qian L, Xie C. The diagnostic performance of quantitative mapping in breast cancer patients: a preliminary study using synthetic MRI. Cancer Imaging 2020;20:88.
20. Arita Y, Takahara T, Yoshida S, Kwee TC, Yajima S, Ishii C, Ishii R, Okuda S, Jinzaki M, Fujii Y. Quantitative Assessment of Bone Metastasis in Prostate Cancer Using Synthetic Magnetic Resonance Imaging. Invest Radiol 2019;54:638-44.
21. Du S, Gao S, Zhang L, Yang X, Qi X, Li S. Improved discrimination of molecular subtypes in invasive breast cancer: Comparison of multiple quantitative parameters from breast MRI. Magn Reson Imaging 2021;77:148-58.
22. Karlo CA, Di Paolo PL, Chaim J, Hakimi AA, Ostrovnaya I, Russo P, Hricak H, Motzer R, Hsieh JJ, Akin O. Radiogenomics of clear cell renal cell carcinoma: associations between CT imaging features and mutations. Radiology 2014;270:464-71.
23. Mahesh M. The Essential Physics of Medical Imaging, Third Edition. Med Phys 2013. doi: 10.1118/1.4811156.
24. Yushkevich PA, Gerig G. ITK-SNAP: An Intractive Medical Image Segmentation Tool to Meet the Need for Expert-Guided Segmentation of Complex Medical Images. IEEE Pulse 2017;8:54-7.
25. Li H, Liu L, Shi Q, Stemmer A, Zeng H, Li Y, Zhang M. Bladder cancer: detection and image quality compared among iShim, RESOLVE, and ss-EPI diffusion-weighted MR imaging with high b value at 3.0 T MRI. Medicine (Baltimore) 2017;96:e9292.
26. Chen H, Chen L, Liu F, Lu J, Xu C, Wang L. Diffusion-weighted magnetic resonance imaging in bladder cancer: comparison of readout-segmented and single-shot EPI techniques. Cancer Imaging 2019;19:59.
27. Wahid KA, Ahmed S, He R, van Dijk LV, Teuwen J, McDonald BA, Salama V, Mohamed ASR, Salzillo T, Dede C, Taku N, Lai SY, Fuller CD, Naser MA. Evaluation of deep learning-based multiparametric MRI oropharyngeal primary tumor auto-segmentation and

investigation of input channel effects: Results from a prospective imaging registry. Clin Transl Radiat Oncol 2021;32:6-14.
28. Pipe JG. Motion correction with PROPELLER MRI: application to head motion and free-breathing cardiac imaging. Magn Reson Med 1999;42:963-9.
29. Ogura A, Maeda F, Miyai A, Kikumoto R. Effects of slice thickness and matrix size on MRI for signal detection. Nihon Hoshasen Gijutsu Gakkai Zasshi 2005;61:1140-3.
30. Zhang K, Liu C, Zhu Y, Li W, Li X, Zheng J, Hong G. Synthetic MRI in the detection and quantitative evaluation of sacroiliac joint lesions in axial spondyloarthritis. Front Immunol 2022;13:1000314.
31. André J, Barrit S, Jissendi P. Synthetic MRI for stroke: a qualitative and quantitative pilot study. Sci Rep 2022;12:11552.

Cite this article as: Li M, Fu W, Ouyang L, Cai Q, Huang Y, Yang X, Pan W, Qian L, Guo Y, Wang H. Potential clinical feasibility of synthetic MRI in bladder tumors: a comparative study with conventional MRI. Quant Imaging Med Surg 2023;13(8):5109-5118. doi: 10.21037/qims-22-1419

